Binding of Proteolytically Processed Phospholipase D from *Streptomyces chromofuscus* to Phosphatidylcholine Membranes Facilitates Vesicle Aggregation and Fusion†

Kimberly A. Stieglitz,‡ Barbara A. Seaton,‡ and Mary F. Roberts*,§

Department of Physiology, Boston University, Boston, Massachusetts 02118, and Merkert Chemistry Center, Boston College, Chestnut Hill, Massachusetts 02467

Received June 26, 2001; Revised Manuscript Received August 31, 2001

ABSTRACT: Ca^{2+}-dependent phospholipase D is secreted from *Streptomyces chromofuscus* as an intact enzyme of 57 kDa (PLD_{57}). Under certain growth conditions, PLD is proteolytically cleaved and activated to form $PLD_{42/20}$ (named for the apparent size of the peptides). The PLD_{42} catalytic core and 20 kDa C-terminal domain remain tightly associated through noncovalent interactions. In the presence of Ba^{2+} (to enhance protein binding to zwitterionic vesicles without hydrolysis of substrate), $PLD_{42/20}$, but not PLD_{57}, induces POPC vesicle leakiness as measured by entrapped CF leakage. $PLD_{42/20}$ also induces vesicle fusion (as measured by light scattering, fluorescence quenching, and cryo-TEM) under these conditions (1 mM POPC, 5 mM Ba^{2+}); neither PLD_{42} nor PLD_{20} alone can act as a fusogen. For intact PLD_{57} to cause CF leakiness, the soluble activator diC_4PA must be present. However, even with diC_4PA, PLD_{57} does not induce significant vesicle fusion. In the absence of metal ions, all PLD forms bind to PC vesicles doped with 10 mol % PA. Again, only $PLD_{42/20}$ is fusogenic and causes aggregation and fusion on a rapid time scale. Taken together, these data suggest that activated $PLD_{42/20}$ inserts more readily into the lipid bilayer than other PLD forms and creates structures that allow bilayers to fuse. Cleavage of the PLD_{57} by a secreted protease to generate $PLD_{42/20}$ occurs in the late stages of *S. chromofuscus* cell cultures. Production of this more active and fusogenic enzyme may play a role in nutrient scavenging in stationary phase cultures.

Phospholipase D (PLD)[1] enzymes are phosphodiesterases that generate phosphatidic acid from phospholipid substrates. They are found in plants, many bacterial species, and a variety of eukaryotic cells and exhibit sequence similarities that are part of a PLD superfamily (*1*). Different types of PLD have different substrate specificity and requirements for divalent cations. In mammalian systems, these enzymes have key roles in signal transduction and membrane trafficking (*2*, *3*). Bacterial PLD enzymes, usually smaller than their mammalian homologues, are often secreted into the media where they may have a primary role in generating organophosphates as a source of phosphate. In some bacteria, PLD has also been suggested as a virulence determinant (*4*, *5*), although whether it is absolutely required for virulence has been debated (*6*, *7*).

Phospholipase D from *Streptomyces chromofuscus* is secreted as an intact protein of 57 kDa. It can be proteolytically processed to a more active form, $PLD_{42/20}$, that is named for the apparent sizes of its two tightly complexed components (*8*). Although its role may be different, *S. chromofuscus* PLD shares with human intracellular PLD a high affinity for anionic lipids that activate the intact protein (*9*). Mammalian PLD is activated by PIP_2 (*10*, *11*), while PLD_{57} from *S. chromofuscus* is activated by its cleavage product phosphatidic acid (*12*). The proteolytically processed $PLD_{42/20}$ is not activated by PA; it also exhibits a 10-fold lower apparent K_m for POPC vesicles than intact protein (*8*). Isolated PLD_{42} is also not activated by PA so that the C-terminal portion of the protein is critical to PA activation (*8*). The activation of this PLD by proteolysis could be important for the role of PLD in *Streptomyces* physiology, either for phosphate retrieval or for infectivity. The latter would clearly involve interactions of the PLD with target membranes and might include changes in membrane structure other than just localized hydrolysis and generation of PA.

This study presents data that correlate the enhanced kinetic activity of $PLD_{42/20}$ with an enhanced ability to disrupt vesicle integrity in the absence of phospholipid hydrolysis. $PLD_{42/20}$, but not the intact PLD_{57} or the isolated N-terminal or C-terminal fragments, is shown to (i) disrupt membrane integrity in the presence of inhibitory Ba^{2+} or diC_4PA (with EDTA present) and (ii) induce fusion of PC SUVs as measured by light scattering, a fluorescence resonance energy transfer vesicle fusion assay, and cryo-TEM.

† This work has been supported by NIH Grant GM 26762 (M.F.R.).

* To whom correspondence should be addressed: phone, (617) 552-3616; fax, (617) 552-2705; e-mail, mary.roberts@bc.edu.

‡ Boston University.

§ Boston College.

[1] Abbreviations: PLD, phospholipase D; PIP_2, phosphatidylinositol 4,5-bisphosphate; CMC, critical micelle concentration; PC, phosphatidylcholine; diC_4PC, 1,2-dibutyroyl-*sn*-glycero-3-phosphocholine; diC_4PA, 1,2-dibutyroyl-*sn*-glycero-3-phosphatidic acid; diC_4PMe, 1,2-dibutyroylphosphatidylmethanol; POPC, 1-palmitoyl-2-oleoyl-*sn*-glycero-3-phosphocholine; POPA, 1-palmitoyl-2-oleoyl-*sn*-glycero-3-phosphate; NBD-PA, 1-palmitoyl-2-[12-[(7-nitro-2,1,3-benzoxadiazol-4-yl)amino]dodecanoyl]-*sn*-glycero-3-phosphate; NBD-PE, *N*-(7-nitrobenz-2-oxa-1,3-diazol-4-yl)-1,2-dihexadecanoyl-*sn*-glycero-3-phosphoethanolamine; Rho-PE, lissamine rhodamine B 1,2-dihexadecanoyl-*sn*-glycero-3-phosphoethanolamine; SUV, small unilamellar vesicle; EM, electron microscopy; cryo-TEM, cryogenic transmission EM.

10.1021/bi011338o CCC: $20.00
Published on Web 10/23/2001

MATERIALS AND METHODS

Chemicals. POPC, POPA, diC$_4$PC, and NBD-PA were purchased from Avanti Polar Lipids, Inc., and used without further purification. The short-chain phospholipids diC$_4$PA and diC$_4$PMe were synthesized as described previously (*13*) from diC$_4$PC using PLD at pH 8.0 or 5.8 (in the presence of 50% methanol), respectively. NBD-PE and Rho-PE were purchased from Molecular Probes. Carboxyfluorescein and Triton X-100 were obtained from Sigma. Hitrap HIC and Hitrap Q columns and bulk resins such as phenyl-Sepharose, Sephadex G-50, and DEAE-Sephadex were purchased from Amersham Pharmacia Biotech.

Generation and Purification of Different PLD Forms. Small amounts of *S. chromofuscus* PLD proteins were prepared from commercially available *S. chromofuscus* PLD obtained from Sigma as described previously (*8*). Larger batches of proteins (more specifically PLD forms that were proteolytically clipped) were isolated from *S. chromofuscus* growth media. *S. chromofuscus* (strain 23616 obtained from ATCC) dried cell pellets were resuspended in ISP-1 medium (DIFCO), streaked on solid agar ISP-2 medium, and grown at 28 °C for 5−7 days. The colonies were individually harvested and added to 10 mL of ISP-1 medium enriched with 1% yeast extract agar (soft gel). The liquid cultures were grown at 30 °C with continuous shaking; these cultures were used to inoculate larger volumes of media. For isolation of the intact enzyme, PLD$_{57}$, 8−10 L of liquid media was harvested 30 h after the onset of growth. To maximize production of the clipped but still associated enzyme, PLD$_{42/20}$, cultures were grown for 48 h after the onset of growth and then harvested. Optimized production of PLD$_{42}$ required incubation of the cultures for 3−4 days after the onset of growth prior to harvesting. The culture medium was concentrated 6-fold and protein precipitated in 60% acetone (w/v) as previously described (*14*). PLD$_{20}$ production was maximal at about 60−70 h after the onset of growth. However, its concentration was variable due to rapid proteolytic degradation. PLD$_{20}$ could also be obtained from PLD$_{42/20}$ as previously described (*8*). Protein concentration was measured using the Lowry method (*15*).

Another source of *S. chromofuscus* (strain NRRL 11098 or A-0848) was obtained from the USDA and also used to generate PLD proteins. That strain was resuspended in 10 mL of T-soy medium (Sigma) and incubated for 3−5 days until growth occurred, transferred (1.5 mL/L) into T-soy broth, and incubated for 40−45 h. This *S. chromofuscus* strain gave reproducible yields of the intact enzyme (PLD$_{57}$) which could then be proteolytically processed by incubating it with concentrated medium from the ATCC strain.

The PLD proteins isolated from Sigma preparations were usually purified with Hitrap HIC and Hitrap Q columns (*8*). For purification of the protein secreted into culture supernatants, larger columns and different resins were used. Chromatography using palmitoylcellulose (a gift from Dr. Nancy Bucher, Boston University) was the most efficient way of purifying PLD$_{57}$ from the culture media at early time points when other fragments were not highly expressed (*14*). This chromatographic step was effective at extracting intact PLD$_{57}$ and separating PLD$_{42}$ and PLD$_{20}$ directly from the culture media (adjusted to pH 7.0). Alternatively, PLD$_{57}$, PLD$_{42}$, and PLD$_{20}$ could be separated using phenyl-Sepharose column chromatography and elution with a gradient of 1.0−0 M NaCl in Tris-HCl, pH 8.0. This step was often carried out twice to prepare pure isoforms of PLD.

Purification of PLD$_{20}$ from ammonium sulfate precipitated media was carried out either (i) using a large (90 × 7.5 cm) Sephadex G-50 column equilibrated with 10 mM Tris-HCl, pH 8.0, or (ii) using a DEAE-Sephadex column (45 × 2.5 cm) and elution with increasing NaCl. Although this last chromatographic step was ineffective at removing small amounts of PLD$_{42}$ associated with PLD$_{57}$, it was very effective at separating PLD$_{20}$ from other PLD protein forms.

Column fractions were analyzed for protein by SDS−PAGE as well as absorption at 280 nm; active PLD forms (PLD$_{57}$, PLD$_{42/20}$, and PLD$_{42}$) were also monitored by a diC$_7$-PC turbidity assay. Aliquots from the column were added to 5 mM diC$_7$PC in 10 mM Tris-HCl, pH 8.0, with 5 mM Ca^{2+}. When ≥10% of the PC was converted to diC$_7$PA, the solution became extremely cloudy; the time until the solution became turbid was a reflection of the amount of active protein.

PLD Intrinsic Fluorescence. Steady-state fluorescence measurements of PLD intrinsic fluorescence were performed with a Shimadzu RF 5000 V spectrofluorometer (with a xenon light source) at 23 °C. The excitation wavelength was 285 nm, with both excitation and emission slit widths set at 1.5 nm. The emission was scanned from 290 to 390 nm. All four PLD species were dialyzed against 10 mM Tris-HCl, pH 8.0, containing 100 mM NaCl and concentrated to 10 μg/mL. After an initial spectrum, Ca^{2+} (10 μM to 50 mM) or diC$_4$PA was added and the fluorescence spectrum monitored as a function of added ligand. The pH of the samples was maintained at 8.0. Ligand-induced shifts in λ_{em} for maximum fluorescence emission were used to estimate a K_D for diC$_4$PA binding to PLD$_{57}$ and PLD$_{42/20}$ using a cooperative model (n = number of interacting sites) for ligand binding. The diC$_4$PA titration was repeated three times with duplicate time points each time. The changes in fluorescence intensity at λ_{em} upon binding Ca^{2+} were used to differentiate high- and low-affinity divalent metal ion binding sites on the different PLD proteins.

Preparation of Small Unilamellar Vesicles. Sonicated POPC vesicles (10 mM final phospholipid concentration) were prepared in buffer (100 mM NaCl, 10 mM Tris-HCl, pH 8.0) in the absence or presence of 6 mM Ba^{2+} and 1 mM EGTA (*9*). A Branson W-350 sonicator was used with a small tip (3.0 cm), 50% duty cycle, pulsing for 5 × 3 min intervals with 1−2 min delay to prevent the solution from overheating. Sonicated POPC/POPA (9:1) vesicles were also prepared in buffer in the absence of Ba^{2+} as described previously (*9*). All steps were done under argon or N_2 to prevent degradation of the vesicles (notably oxidation of the POPC double bonds). These small unilamellar vesicle (SUV) preparations were periodically monitored before and after sonication by extracting the lipids in organic solvent, drying the extract by rotary evaporation, resuspending the film in organic solvent (CD_3OD), and acquiring ^{31}P NMR (202.3 MHz) spectra [using a Varian INOVA 500 and parameters described previously (*8*, *9*)] or analyzing the mixture by thin-layer chromatography on silica gel G (Alltech) to check for hydrolysis. The TLC plates were developed with chloroform/methanol/acetic acid/water (50:30:8:4) to separate PC, lysoPC, and phosphatidic acid (*16*). Final phospholipid

content was determined by the ashing procedure for total phosphate (*17*).

Vesicle Leakage Assays. PLD binding to vesicles could cause leakage, aggregation, or fusion. To monitor leakiness promoted by the bound proteins, sonicated vesicles were prepared with entrapped, self-quenched CF (150 mM) in 50 mM Hepes, pH 7.5, in the presence and absence of 10 mM Ba^{2+}. Unentrapped CF was removed by passage of the vesicle solution through a Sephadex G-10 column (0.9 × 20 cm) preequilibrated with Hepes, pH 7.5. Vesicle integrity in the absence or presence of PLD proteins and divalent cations as well as diC_4PA under conditions where binding of the enzymes occurs without PC hydrolysis was monitored by the CF fluorescence at 520 nm. Increased fluorescence intensity at 520 nm (measured 15 min after addition of PLD) indicates release of vesicle-trapped CF into the bulk solution. The addition of 5 mM Ba^{2+} or diC_4PA to the POPC vesicles with entrapped CF did not cause any detectable leakage (as measured by increased fluorescence) in the absence of PLD. As a control for complete leakage of CF, the vesicles were mixed with Triton X-100 (1 vol %). The addition of the detergent caused a 200−300-fold increase in emission (depending on how well the free CF was removed from the sample).

Vesicle Aggregation/Fusion Assays. Three types of assays, (i) NBD-PA self-quenching, (ii) solution turbidity at 350 nm, and (iii) NBD-PE/Rho-PE resonance energy transfer, were used to assess the ability of the PLD and fragments to induce PA clustering and vesicle aggregation and fusion under conditions where binding of the proteins occurs. The fluorescence intensity of NBD-PA (100 μM) doped in POPC (1 mM) vesicles will become self-quenched if the PA becomes clustered together rather than randomly distributed in the plane of the bilayer or if vesicles aggregate (enhanced proximity of PA molecules in different vesicles). The effect of PLD proteins (and Ba^{2+}) on the NBD-PA fluorescence was monitored at 530 nm every 2 min for the first 15 min and then again at 30 min for a final intensity after addition of the protein using a Perkin-Elmer L5-5B luminescence spectrometer with an excitation wavelength of 465 nm. Data points were measured in triplicate with an average error <10%.

Aggregation and/or fusion of the POPC vesicles promoted by PLD was monitored by the increase in turbidity of the lipid suspension after addition of the protein (*18*). The solution optical density at 350 nm was measured with a Perkin-Elmer Lambda 2 UV/vis spectrophotometer; the baseline turbidity was provided by monitoring OD_{350} of POPC vesicles without protein ($OD_{350} = 0.06 \pm 0.01$). Ba^{2+} (5 mM diluted from a 0.5 M stock) was then added to the vesicle suspension (it had no effect on OD_{350}), followed by the different PLD proteins (PLD_{57}, $PLD_{42/20}$, PLD_{42}, and PLD_{20}). As a control for fusion produced by small amounts of POPA in the POPC vesicle, separate SUVs composed of 10 mM POPC and 0.05 or 0.10 mM POPA were prepared, and the ΔOD_{350} was monitored over 15 min. These amounts of PA represent conservative estimates for the lower threshold of PLD products that could be detected by TLC. Upon the addition of 5 mM Ba^{2+} there was no change to the sample with 0.05 mM POPA; the sample with 0.1 mM POPA showed an increase of 0.05 at OD_{350} within the first 3 min that did not change any further. To distinguish vesicle fusion from aggregation, EDTA (5 mM) was added to the suspensions at various times after the addition of PLD proteins. Reversible optical density changes represent vesicle aggregation; irreversible turbidity increases indicate fusion.

A fluorescence resonance energy transfer assay was also used to monitor vesicle fusion in POPC and POPC/Ba^{2+} vesicles. Vesicles were prepared with 50 μM amounts of two types of fluorescently tagged phosphatidylethanolamines, NBD-PE and Rho-PE, each doped in 10 mM POPC. A mixture of the two types of SUVs was incubated with either PLD_{57}, $PLD_{42/20}$, or PLD_{42} in the absence or presence of Ba^{2+}. The NBD fluorescence intensity at 530 nm was measured every 10 s for 15 min and then again at 30 min as a final time point. Fusion causes a net decrease in donor fluorescence and increase in acceptor (Rho-PE) fluorescence (*19*); aggregation without fusion would have little effect on the NBD-PE or Rho-PE fluorescence. The experiments were run in triplicate for both PLD_{57} and $PLD_{42/20}$.

Dynamic Light Scattering. Dynamic light scattering measurements of vesicle sizes were carried out in triplicate on 2.5 mL samples (in plastic cuvettes) with a Coulter N4 system at a temperature of 24−25 °C. Sampling times were 1−3 min; diameters (measured for each vesicle sample in triplicate) are reported with standard deviations in the mean. POPC vesicles prepared for DLS were spun in a microfuge for 1 h in the cold at top speed to eliminate aggregates or giant vesicles prior to the experiment. A population of LUVs (average diameter from 72 to 82 nm) was isolated from SUVs by this procedure. These LUVs were used for DLS measurements of the effect of PLDs on larger vesicles. POPC-sonicated vesicles were stable for up to 24 h in the absence of Ba^{2+} in the binding buffer. For POPC vesicles with Ba^{2+} analyzed within 2 h of preparation, less than 5% of the vesicles had diameters >450 Å.

Electron Microscopy. Negative staining EM (using 1% sodium tungstate) of vesicles in the absence and presence of PLD forms was used to screen preparations prior to cryo-TEM (which were carried out with a calibrated Philips CM-12 transmission electron microscope). An aliquot (4 μL) of vesicles in binding buffer (6−7 mg of lipid/mL of solution) was placed on carbon-coated, glow-discharged grids for 10 s at room temperature. The grids were briefly washed with distilled water five times and blotted. For negative staining EM the grids were incubated with sodium tungstate for 1−3 min and then blotted to air-dry. Cryo-TEM was used to obtain accurate sizes and distributions of sizes for vesicles incubated for 15 min with $PLD_{42/20}$. Samples (grids containing vesicles) were flash frozen in a liquid ethane bath at less than −80 °C (the very rapid cooling preserves microstructures). The vitrified specimen was placed in an cryogenic grid holder stored below −80 °C. Samples (two for POPC vesicles alone and one each for POPC/Ba^{2+} and POPC/Ba^{2+}/$PLD_{42/20}$ but each used to prepare six to eight grids) were imaged with 100 kV electrons at a magnification of 45000×. Diameters of over 500 vesicles were measured in this fashion (∼130 per sample). The cryo-TEM analysis showed no significant aggregation or fusion of POPC vesicles with or without Ba^{2+} in the absence of PLD. However, vesicles had to be used within 6 h of preparation. Preparations of vesicles with Ba^{2+} that were older than 6−8 h or stored at 4 °C showed an increased population of vesicles with a diameter of >700 Å. Careful examination of the electron micrographs

showed that the particles in this size range were most often aggregates of two or three vesicles.

RESULTS

Production of PLD by S. chromofuscus. Inoculation of the ATCC strain (23616) of *S. chromofuscus* in liquid media at 28 °C led to visible growth within 8−12 h. Once growth was evident, cultures increased in mass rapidly. Within 30 h, intact PLD_{57} could be detected by SDS−PAGE with standard Coomassie staining when the medium was concentrated 100−150-fold. The concentration of PLD in the medium was estimated between 0.1 and 0.5 μg/mL. Within 48 h, large "clumps" of cells began to form, and these increased in size for an additional 2−3 days. Further increases in cell mass were much slower after 48 h. At 48 h, the proteolytically clipped form of the enzyme could be observed; appearance of the more active $PLD_{42/20}$ correlated with cell "clumping". After 3−4 days, PLD_{42} was one of the major proteins in the culture along with PLD_{20}. The regulation of protein secretion in *S. chromofuscus* is not well understood. However, the pattern of PLD expression was very sensitive to temperature changes. Increasing the growth temperature to 30 °C led to increased initial growth and many more bands detected by SDS−PAGE for secreted proteins. For the purpose of harvesting the maximum amount of PLD fragments, most of the cultures were grown at 30 °C for 2−3 days. Under optimal growth conditions after growth for 2 days, 8−10 L of inoculated media characteristically produced 1.5−3.0 mg of PLD_{57}, 3.0−4.0 mg of $PLD_{42/20}$, and 1−2 mg of PLD_{42}. After 4 days, there was less than 1.0 mg of PLD_{57}, 1−2 mg of $PLD_{42/20}$, 2−4 mg of PLD_{42}, and 1−2 mg of (intact) PLD_{20}.

Effect of Ligands on PLD Intrinsic Fluorescence. The intrinsic fluorescence spectra of different PLD forms were obtained in 10 mM Tris-HCl and 1 mM EGTA, pH 8.0 (Figure 1A). PLD_{57} exhibits a maximum fluorescence intensity, λ_{max}, at 357 nm. In contrast, both $PLD_{42/20}$ and PLD_{42} have maxima shifted to 335 nm. PLD_{57} has 13 tryptophans, so a more detailed analysis of the intrinsic fluorescence is not possible. However, there are clearly environmental differences for one or more fluorophores consistent with proteolytic cleavage generating a more hydrophobic environment for at least one of the fluorophores. The intrinsic fluorescence of the proteins is also sensitive to ligand binding and can be used to estimate ligand binding affinities.

Ca^{2+} is a key ligand for this PLD. Amounts of Ca^{2+} less than 0.5 mM are necessary for PLD to catalyze the hydrolysis of monomer substrate [a Ca^{2+} $K_D = 75$ μM is extracted from kinetics using diC_4PC (*8*)], whereas for PA activation toward PC vesicle substrates, a phenomenon dependent on the presence of the 20 kDa domain (*8*), 5 mM Ca^{2+} is required for optimal Ca^{2+} (the exact value depends on the mole fraction of PA and bulk concentration of phospholipid). These kinetic requirements of the enzyme for Ca^{2+} are mirrored in changes in the intrinsic fluorescence spectrum of PLD induced by calcium ions (Figure 1B). The presence of Ca^{2+} did not alter λ_{max} for any of the PLD forms. However, Ca^{2+} had a profound effect on intrinsic fluorescence intensity. Both PLD_{57} and $PLD_{42/20}$ displayed a biphasic change in fluorescence intensity as increased amounts of Ca^{2+} were

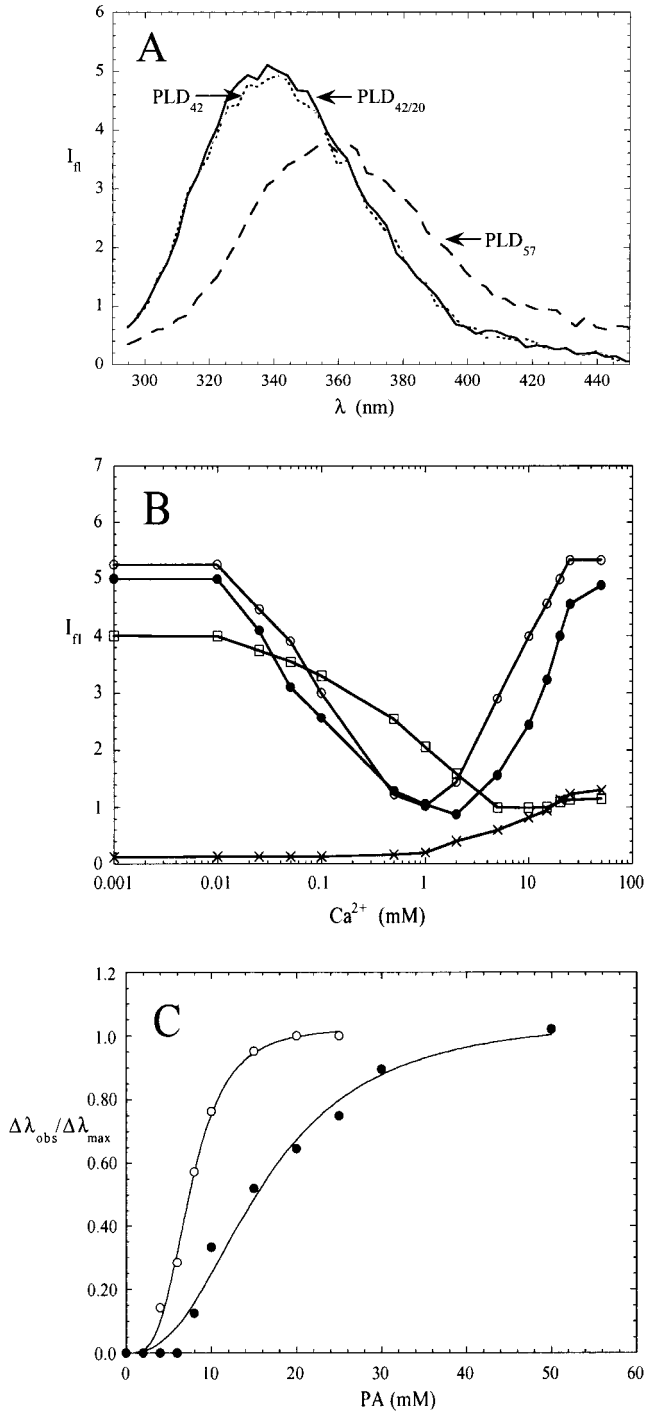

FIGURE 1: (A) Intrinsic fluorescence spectra of (- - -) PLD_{57} (10 μg/mL), (—) $PLD_{42/20}$ (10 μg/mL), and (•••) PLD_{42} (10 μg/mL). (B) Effect of Ca^{2+} on the intrinsic fluorescence of different PLD forms (each at 10 μg/mL): ○, PLD_{57}; ●, $PLD_{42/20}$; □, PLD_{42}; ×, PLD_{20}. (C) Fractional change in emission λ_{max} of PLD_{57} (○) and $PLD_{42/20}$ (●) as a function of diC_4PA concentration. The data were fit with a hyperbolic cooperative binding model.

added. Initially, there was a decrease in intensity (up to 1 mM Ca^{2+}) followed by an increase as the Ca^{2+} was further increased. Figure 1B shows one such titration for each PLD protein; three such titrations were performed. The average calcium concentration needed for half the total drop in fluorescence, $[Ca^{2+}]_{0.5}$, was determined to be 0.075 ± 0.012 mM for PLD_{57} and 0.08 ± 0.01 mM for $PLD_{42/20}$. These $[Ca^{2+}]_{0.5}$ values are similar to the kinetic K_D for Ca^{2+} determined with diC_4PC as substrate (*8*). Similar $[Ca^{2+}]_{0.5}$

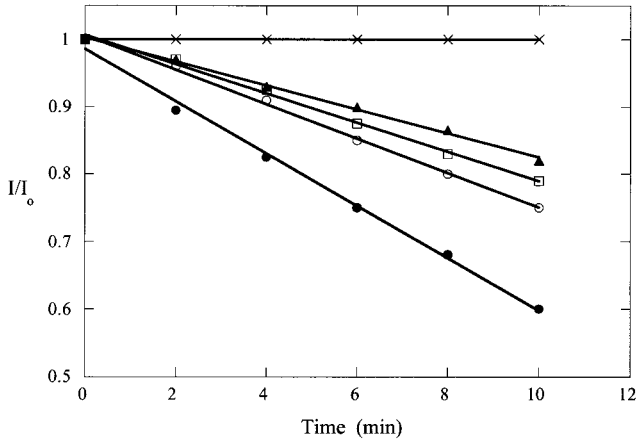

FIGURE 2: Quenching of NBD-PA fluorescence in PC vesicles in 10 mM Tris-HCl and 1 mM EDTA, pH 8.0, upon the addition of PLD forms: (A) ○, 150 μg of PLD_{57}; ●, 150 μg of $PLD_{42/20}$; □, 150 μg of PLD42; ×, 300 μg of PLD_{20}. For comparison, the effect of 5 mM Ba^{2+} and no PLD is shown (▲).

values can be extracted for the Ca^{2+} binding that subsequently increases the intrinsic fluorescence: 3.3 ± 1.2 and 12.5 ± 0.2 mM for PLD_{57} and $PLD_{42/20}$, respectively. In contrast, isolated PLD_{42} and PLD_{20} exhibited a simple single-phase response as Ca^{2+} increased from micromolar to millimolar amounts. The intrinsic fluorescence of PLD_{42} decreased in intensity as Ca^{2+} increased ($[Ca^{2+}]_{0.5} = 0.42 \pm 0.08$ mM); PLD_{20} intrinsic fluorescence increased in the millimolar range ($[Ca^{2+}]_{0.5} = 8.5 \pm 0.9$ mM). This behavior indicates that high-affinity Ca^{2+} binding sites affecting tryptophan residues are on the catalytic core of PLD_{57}, $PLD_{42/20}$, or PLD_{42} and low-affinity calcium binding sites near appropriate fluorophores are on the PLD_{20} fragment.

In contrast to the effects of Ca^{2+}, the soluble allosteric activator diC_4PA (in the presence of EGTA) had no effect on the protein fluorescence intensity but did cause a shift in λ_{max} when bound to both PLD_{57} (λ_{max} blue shifted from 356 to 335 nm) and $PLD_{42/20}$ (λ_{max} red shifted from 335 to 359 nm). The dependence of the fractional changes in λ_{max} as a function of diC_4PA concentration was fit with a cooperative binding model to estimate a K_D for diC_4PA binding to the proteins (Figure 1C): 7.5 ± 0.2 mM ($n = 3.6 \pm 0.3$) and 16.0 ± 1.4 mM ($n = 2.5 \pm 0.4$) for diC_4PA binding to PLD_{57} and $PLD_{42/20}$, respectively. The high binding constant of diC_4-PA for PLD_{57} is consistent with the observation that this soluble activator was much less effective than long-chain PA in binding PLD_{57} to a PC membrane (*9*).

Effect of PLD on Clustering/Aggregation of NBD-PA. It has been proposed that PA clustering in a PC membrane is related to kinetic activation (*12*). Divalent cations, e.g., 5 mM Ba^{2+}, induce PA aggregation in a PC bilayer as monitored by self-quenching of the NBD-PA (Figure 2, triangles). However, PLD in the absence of divalent cations could also affect the distribution of PA. To test this, PLD proteins were added to PC/NBD-PA (10:1) vesicles under conditions (1 mM EDTA and no added metal ions) where they bound to the vesicles without any PC hydrolysis. In Figure 2 are shown the data for the first 10 min after addition of PLD; the decrease in fluorescence was linear with time during this period. $PLD_{42/20}$ was clearly the most effective at causing quenching of NBD-PA fluorescence under these conditions. Both PLD_{57} and PLD_{42} were less effective but

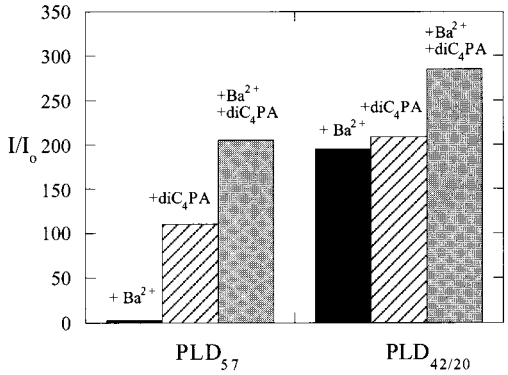

FIGURE 3: Effect of added PLD_{57} and $PLD_{42/20}$ (both at 150 μg/mL) on the fluorescence of POPC-entrapped CF in the presence of 5 mM Ba^{2+} or 10 mM diC_4PA and then in the presence of both Ba^{2+} and diC_4PA.

could also induce NBD-PA quenching. PLD_{20} was totally ineffective at inducing NBD-PA quenching even though this fragment binds tightly to PC/PA vesicles in the absence of divalent cations (*9*). Thus, PLD fragments containing the active site bound to PC/PA vesicles and induced clustering of the PA in the absence of divalent cations. The extent of the clustering was significantly greater than that produced by divalent cations alone only with intact PLD_{57} and $PLD_{42/20}$.

PLD-Enhanced Leakiness of SUVs. The ability of the PLD proteins bound to PC in the presence of Ba^{2+} to affect vesicle leakiness was assessed by monitoring the fluorescence of entrapped CF. POPC vesicles containing CF had negligible fluorescence intensity that did not increase over a 3 h period. Within minutes after adding $PLD_{42/20}$, a significant increase in CF fluorescence intensity was observed; the same amount of PLD_{57} added to the vesicles had no effect on CF fluorescence (Figure 3). In the presence of diC_4PA instead of Ba^{2+}, both $PLD_{42/20}$ and PLD_{57} were able to induce CF leakage from the POPC vesicles, although the clipped PLD caused greater leakiness. In the presence of both Ba^{2+} and diC_4PA, both enzyme forms caused significant loss of entrapped CF. Since both PLD forms are bound to PC bilayers in the presence of Ba^{2+}, there must be a difference in the mode of binding of intact versus proteolytically clipped PLD such that the clipped protein is more disruptive.

$PLD_{42/20}$ Promotes Aggregation/Fusion of POPC/Ba^{2+} Vesicles. The vesicle aggregation/fusion assay that monitors solution optical density was carried out under conditions where divalent cation dependent binding of PLD species occurs (*9*). Incubation of the four PLD species, PLD_{57}, PLD_{42}, $PLD_{42/20}$, and PLD_{20}, at 300 μg/mL with POPC vesicles and 5 mM Ba^{2+} clearly showed that neither PLD_{20} nor PLD_{42} was able to increase the solution turbidity of POPC vesicles (Figure 4A). PLD_{57} promoted a small increase in OD_{350} within the first minute (from 0.06 to 0.13), while $PLD_{42/20}$ generated significantly more light scattering over a longer time period (from 0.06 to 0.36). This indicates that neither the catalytic core, PLD_{42}, nor the 20 kDa C-terminal PA activation domain is sufficient to induce aggregation/fusion of SUVs even though these proteins are bound to the vesicles. Furthermore, the intact PLD molecule is less effective than the proteolytically clipped protein. The increased sample turbidity mediated by $PLD_{42/20}$ depended on the concentration of the enzyme (Figure 4B) and was reversible if EDTA was added at early time points (Figure

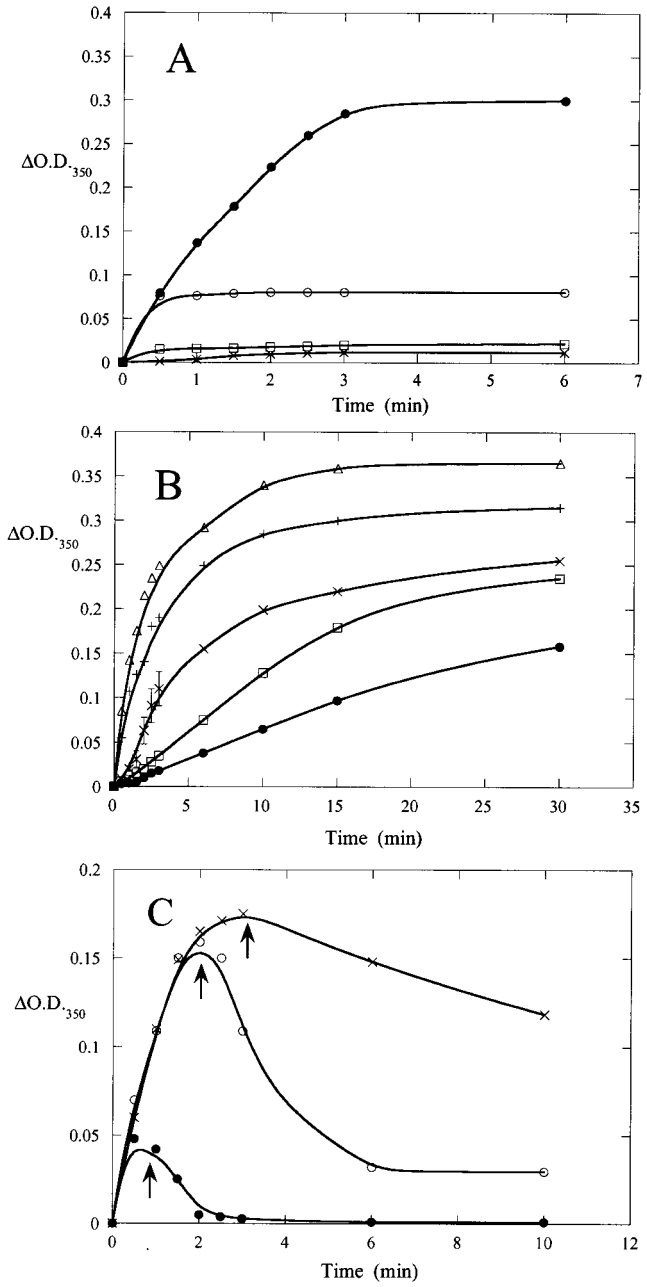

FIGURE 4: (A) Turbidity (OD_{350}) of a 10 mM POPC SUV preparation (5 mM Ba^{2+} present) upon the addition of 300 μg/mL PLD forms: ○, PLD_{57}; ●, $PLD_{42/20}$; □, PLD_{42}; ×, PLD_{20}. (B) Effect of different concentrations (μg/mL) of $PLD_{42/20}$ on the vesicle solution turbidity: ●, 25; □, 50; ×, 75; +, 150; △, 300. (C) Effect of EDTA on the turbidity changes of the POPC/Ba^{2+} SUV preparation after the addition of 150 μg/mL $PLD_{42/20}$. The arrows indicate when 5 mM EDTA was added to the solution.

4C). The increase in light scattering was completely reversed if EDTA (5 mM) was added 1 min after the addition of the enzyme. However, when EDTA was added 3 min after the incubation of the vesicles with protein, most of the increased light scattering was irreversible. For PLD_{57}, the small increase in solution turbidity was reversible even when the EDTA was added 15 min after the sample was mixed with $PLD_{42/20}$. The enhanced turbidity of the PC vesicle solution after the addition of $PLD_{42/20}$ and Ba^{2+} and the loss of reversibility with incubation time are suggestive of vesicle fusion, while the reversible scattering induced by PLD_{57} is consistent with

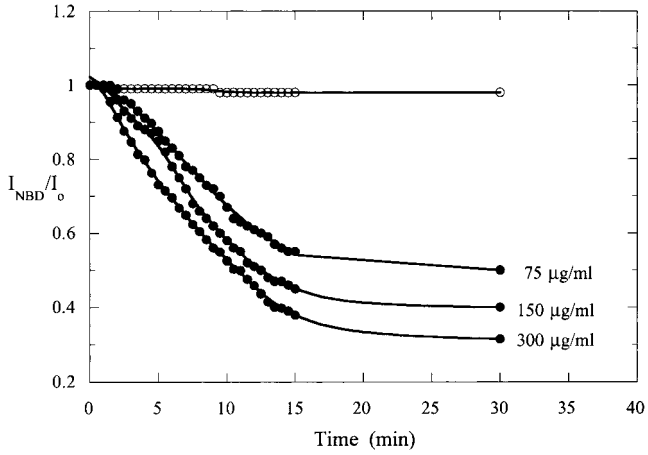

FIGURE 5: Effect of different PLD forms on the resonance energy transfer of fluorescence from NBD-PE to Rho-PE in a mixture of NBD-PE/POPC and Rho-PE/PC vesicles in the presence of 5 mM Ba^{2+}: ○, 300 μg/mL PLD_{57}; ●, $PLD_{42/20}$ (75−300 μg/mL as indicated on the graph).

intact enzyme inducing some vesicle aggregation without fusion.

A resonance energy transfer (RET) assay using separate populations of PC/NBD-PE and PC/Rho-PE vesicles was used to probe for $PLD_{42/20}$-induced vesicle fusion. The NBD-PE moiety was excited and its emission intensity measured in the absence and presence of either PLD_{57} or $PLD_{42/20}$. Quenching of the NBD fluorescence indicates the Rho-PE and NBD-PE are in close proximity. While vesicle aggregation may contribute to a small decrease in NBD fluorescence, via light scattering, only when hemifusion (allowing outer monolayer lipid exchange between vesicles) or full fusion occurs is there efficient RET from the NBD donor to the rhodamine acceptor (*20*). PLD_{57}, which induced quenching of NBD-PA molecules in PC vesicles and caused a small increase in PC vesicle solution turbidity in the presence of Ba^{2+}, had no effect on the NBD-PE fluorescence in this RET fusion assay (Figure 5). Similarly, no decrease in NBD fluorescence was observed when PLD_{42} or PLD_{20} was added to the mixed population of vesicles. However, when the labeled PE/POPC vesicles were incubated with $PLD_{42/20}$ (and Ba^{2+}), there was a concentration-dependent decrease in NBD (donor) fluorescence consistent with fusion of PC/NBD-PE and PC/Rho-PE vesicles (Figure 5).

Light Scattering Analysis of Vesicle Sizes in the Presence of PLD. Dynamic light scattering (DLS) measurements were used to quantify changes in the size distribution of phospholipid vesicles. POPC (or POPC/POPA, 9:1) vesicles prepared without Ba^{2+} were characterized as a mixed population of small unilamellar vesicles with average diameters between 25 and 35 nm. Inclusion of Ba^{2+} increased the average diameter of POPC SUVs to 35 ± 5 nm (Table 1). Sonicated preparations also had a small additional population of vesicles with average diameters between 70 and 80 nm that could be separated from the smaller SUVs by centrifuging the sample at maximum speed in a microfuge (1 h at 4 °C) (*21*). Inclusion of Ba^{2+} had little effect on the average diameters of these vesicles.

The average diameters of POPC/Ba^{2+}, POPC/POPA (molar ratio 9:1), and POPC/diC_4PA SUV vesicle mixtures were characterized in the presence of PLD fragments. Both the SUV population between 30 and 40 nm (Table 1) and

Table 1: Average POPC (10 mM) and POPC/POPA (9 mM:1 mM) Vesicle Diameters (Determined by Dynamic Light Scattering) after Incubation with PLD Forms under Conditions That Promote Protein Binding but without PC Hydrolysis

PLD	μg/mL	additive			vesicle diameter[a]		t[d] (min)
		Ba^{2+}[b]	POPA	diC_4PA[c]	D_-(nm)	D_+(nm)	
PLD_{57}	75	+	−	−	30 ± 4	34 ± 4	17
	150	−	+	−	28 ± 6	24 ± 6	102
	150	−	−	+	35 ± 6	42 ± 6	102
$PLD_{42/20}$	75	+	−	−	30 ± 4	55 ± 4	17
	150	−	+	−	28 ± 8	42 ± 10	51
	300	−	−	+	25 ± 5	46 ± 5	51
PLD_{42}	75	+	−	−	30 ± 5	32 ± 5	17
PLD_{20}	75	+	−	−	30 ± 5	30 ± 5	17
	150	−	+	−	27 ± 6	26 ± 6	102

[a] D_- is the average diameter in the absence of PLD; D_+ is the average diameter after incubation (for the time indicated) with PLD. Standard deviations for each condition are provided. [b] 5 mM Ba^{2+} added. [c] 10 mM diC_4PA added to PC vesicles. [d] Incubation time.

Table 2: Summary of the Effect of Different PLD Forms on Vesicle Properties

property	PLD_{57}	$PLD_{42/20}$	PLD_{42}	PLD_{20}
clustering of NBD-PA[a]	+	++	+	−
PC vesicle leakiness[a]				
$+Ba^{2+}$	−	++		
$+diC_4PA$	+	++		
$+Ba^{2+}$ and diC_4PA	++	+++		
increased solution turbidity	+	+++	−	−
reversibility of turbidity changes	+[b]	−[c]		
fusion				
phospholipid RET	−	+	−	−
DLS	−	+	−	−
cryo-TEM		+		

[a] The number of plus signs indicates the relative extent of NBD-PA clustering or PC vesicle leakiness induced by a given PLD form. [b] Intact PLD causes a very small (but reproducible) increase in solution turbidity that is completely reversible. [c] The changes in solution turbidity are only completely reversible within the first 2 or 3 min.

the larger 70−80 nm vesicle aggregates (data not shown) were not significantly affected by any concentration of PLD_{57} examined (75 and 150 μg/mL). Under these conditions, a significant amount of the PLD_{57} (>70%) should be partitioned onto the vesicles (*9*). Due to the low availability of the PLD_{42} and PLD_{20} fragments, only 75 μg of protein/mL was used for each triplicate time point. PLD_{57} had no statistically significant effect on the average vesicle size under any conditions tried, including the presence of POPA in the SUVs, incubation of PC vesicles with Ba^{2+}, or addition of diC_4PA to the PC/Ba^{2+} SUVs. Similarly, the separate PLD fragments also did not cause any significant change in average vesicle sizes (Table 1).

However, at all three concentrations tested, $PLD_{42/20}$ clearly induced a dose-dependent increase in average diameter of the POPC/Ba^{2+} SUVs. The average diameter increased 1.8-fold when PLD was incubated with POPC SUVs in the presence of Ba^{2+} or diC_4PA and 1.5-fold when the enzyme was incubated with POPC/POPA vesicles in the absence of Ba^{2+}. An increased average size was observed for the larger vesicles as well, although the fraction change in diameter was much smaller (hence most incubations were carried out with SUVs). With 500 μg of $PLD_{42/20}$, the average diameter increased from 75 ± 5 to 90 ± 5 nm 10 min after addition of the enzyme and to 110 ± 5 nm after 17 min. The increased scattering did not reflect hydrolysis of PC to form PA and subsequent fusion induced by Ba^{2+}. TLC analyses of PC/Ba^{2+}/$PLD_{42/20}$ vesicle samples could not detect any PA until 1−1.5 h after incubation with 500 μg/mL protein and 3 h incubation with 300 μg/mL $PLD_{42/20}$. The minimum detectable amount of PA we would see in these samples would correspond to 50 μM. However, vesicles with that amount of product (10 mM POPC/0.05 mM POPA) exhibited no fusion upon the addition of 5 mM Ba^{2+} on the time scales examined here. The proteolytically clipped protein also caused an increase in SUV diameter of POPC/POPA vesicles in the absence of metal ions and POPC vesicles with diC_4-PA added. However, in the absence of Ba^{2+}, only very small increases in the diameter of the larger population of vesicles (75 ± 5 nm prior to addition of protein) were detected when PA, long or short chain, anchored the $PLD_{42/20}$ to the bilayer (150 μg of $PLD_{42/20}$ increased the average diameter of POPC/POPA vesicles to 78 nm; the same amount of enzyme increased the average diameter of POPC vesicles with diC_4-PA added to 83 nm).

Cryo-TEM Analysis of POPC Vesicle Sizes in the Presence of $PLD_{42/20}$. The observations that only $PLD_{42/20}$ caused large irreversible increases in light scattering at 350 nm, decreased NBD-PE donor fluorescence when mixed with separate NBD-PE and Rho-PE containing vesicles, and increased the average diameter of SUVs as measured by DLS (see Table 2 for a summary of how vesicle properties are affected by the different PLD forms) are consistent with that form of *S. chromofuscus* PLD acting as a fusogen. The increased diameter measured by DLS does not prove fusion has occurred nor does it quantify the number of particles in each size range but rather reports scattering events which are more prominent for larger particles. Therefore, as a definitive measure of fusion and for a more accurate analysis of the distribution of particles, vesicle samples were analyzed by cryo-TEM. Careful examination of the electron micrographs of initial vesicle preparations revealed a unilamellar population of vesicles with most of the diameters from 25 to 45 nm with a consistent although relatively small population of clumps of two or three deformed smaller vesicles. These diameters of the clumps were consistently between 70 and 80 nm and were slightly more prominent in vesicle preparations done in the presence of Ba^{2+} that were examined for more than 6 h after preparation. In each micrograph, less than 2% of the vesicles had diameters <200 nm; a few large unilamellar vesicles with diameters greater than 500 nm were also detected.

The population of clumped vesicles and LUVs was separated from the smaller SUVs by centrifugation (*21*). Processing of the vesicles for cryo-TEM within 2 h of preparation also eliminated most of the clumped vesicle sizes. The vesicle suspension was reassayed to get an accurate final concentration of phospholipid (*17*). POPC vesicles prepared in the presence and absence of Ba^{2+} had similar size distributions (Figure 6A,C). In the absence of Ba^{2+} nearly 90% of the population of vesicles had diameters between 25 and 40 nm; the mean vesicle diameter was 32.2 nm with a standard deviation of 1.9 nm. POPC vesicles prepared with Ba^{2+} showed a slightly broadened distribution with 86% of the population between 25 and 40 nm (mean diameter of 33.5 ± 2.2 nm). Thus, the presence of 5 mM Ba^{2+} alone did

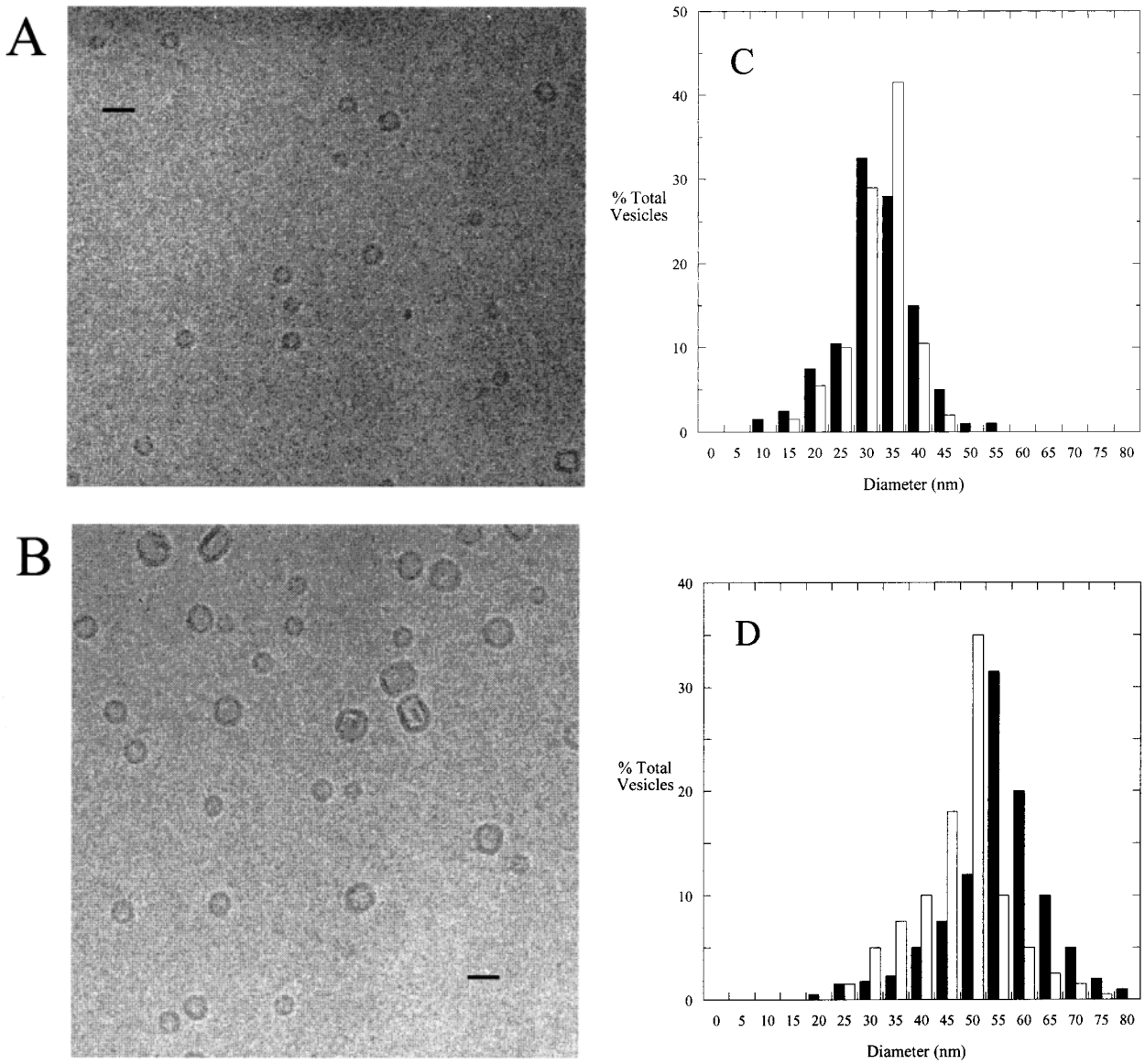

FIGURE 6: Cryogenic transmission electron micrographs of POPC SUVs prepared with 5 mM Ba^{2+} and then incubated for 15 min in the (A) absence or (B) presence of 300 μg/mL $PLD_{42/20}$. The bar on each micrograph is equal to 500 Å. (C) Distribution of POPC SUV diameters in the absence (□) and presence (■) of Ba^{2+}. (D) Effect of $PLD_{42/20}$ incubation on the distribution of POPC vesicle diameters: ■, incubation with $PLD_{42/20}$ and 5 mM Ba^{2+} for 15 min; □, incubation with $PLD_{42/20}$ that had been preincubated with Ba^{2+}(final Ba^{2+} <0.5 mM) for 30 min.

not cause significant changes in the POPC vesicle size distribution.

When the same POPC vesicles (10 mM) prepared in the presence of Ba^{2+} were incubated with 300 μg/mL $PLD_{42/20}$ for 15 min, there was a 60−70% increase in mean vesicle diameters (Figure 6B,D). For this population the mean diameter was 54.8 ± 2.2 nm. The POPC vesicles prepared in the absence of metal ions and then incubated for 30 min with a $PLD_{42/20}$ solution preincubated in 5 mM Ba^{2+} in buffer also exhibited an increase in the mean diameter to 45.6 ± 2.4 nm (Figure 6D). The larger increase in mean diameter corresponds to fusion of about four vesicles. $PLD_{42/20}$ is inactive in these preparations, and the lack of POPC hydrolysis to POPA by $PLD_{42/20}$ was confirmed by ^{31}P NMR analysis of vesicles after incubation with enzyme. That the Ba^{2+} sufficiently inhibited the enzyme (*S. chromofuscus* PLD has an absolute requirement for Ca^{2+} for catalysis) was also confirmed by incubating the enzyme/vesicle preparation with an excellent short-chain phospholipid substrate, diC_4PC, and monitoring via pH stat for any acid production due to product diC_4PA (none was detected). Thus, the changes in vesicle diameter induced by $PLD_{42/20}$ are not due to the production of product PA, which could promote vesicle fusion in the presence of divalent cation, but the result of protein-induced vesicle fusion. These data indicate that the proteolytically activated $PLD_{42/20}$ acts as a fusogen.

DISCUSSION

S. chromofuscus PLD proteins (intact, proteolytically clipped, and isolated fragments) can be bound to PC vesicles under a variety of conditions where no hydrolysis of substrate occurs (*9*). However, there is a clear difference in how the different forms of the enzyme interact with the bilayer as shown by the diverse studies carried out in this work and summarized in Table 2. Proteolytically activated $PLD_{42/20}$ clearly has more disruptive interactions with PC bilayers than any of the other forms of the enzyme. When bound to PC vesicles with Ba^{2+}, only $PLD_{42/20}$ causes loss of entrapped

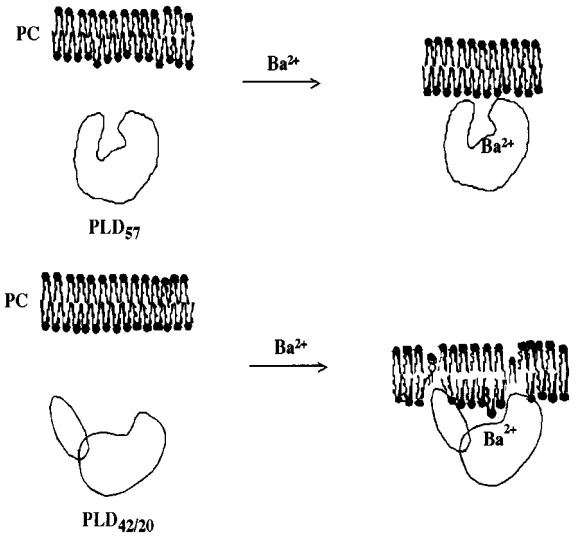

FIGURE 7: Schematic view of interactions of PLD_{57} versus $PLD_{42/20}$ with a PC bilayer in the presence of Ba^{2+}.

solute, increases light scattering and particle size, and increases RET between separate vesicles with donor and acceptor probes. These disruptive interactions of $PLD_{42/20}$ with a PC surface correlate with the kinetic activation (enhanced apparent V_{max} and lower apparent K_m for PC vesicles as substrate) observed previously for $PLD_{42/20}$ compared to PLD_{57} (*12*). That *S. chromofuscus* generates $PLD_{42/20}$ in the medium at later times in cell growth (where it correlates with the clumping morphology of the cells) may suggest that the clipped PLD is critical for supplying the cells with nutrients by disrupting the membranes of any available organisms.

All PLD forms interact tightly with the lipid bilayer through direct binding to anionic lipids (*9*). While Ca^{2+} lessens the affinity of PLD for anionic lipids such as PA, it also clusters the anionic lipids on the membrane surface. PLD_{57}, $PLD_{42/20}$, and PLD_{42} but not PLD_{20} also cluster PA in the absence of divalent metal ions, although the clipped form of the enzyme is the most effective at inducing PA clustering in terms of the rate of clustering. This suggests that there is something about the catalytic core of the enzyme, possibly a patch of cationic residues, that renders it able to aggregate anionic lipids. In contrast to the catalytic core, the C-terminal fragment contains the highest fraction of anionic residues (13%). However, the observation that the intact enzyme, PLD_{57}, also aggregates NBD-PA in POPC vesicles in the absence of Ba^{2+} but does not increase the average diameter suggests that the interactions of PLD that promote PA clustering are not sufficient for vesicle fusion.

For PA activation of PLD_{57} to occur, intact PLD_{57} needs 5 mM Ca^{2+}, a value in the same concentration range as the K_D for the low-affinity Ca^{2+} binding site detected by intrinsic fluorescence of PLD_{57} (the high-affinity Ca^{2+} binding sites that quench PLD intrinsic fluorescence are associated with the catalytic fragment, PLD_{42}). The PA cluster is likely to form a docking site for the PLD_{57}/divalent cation complex. This "activated" PLD_{57} is now bound to the target membrane such that it induces cell leakage as well as optimally hydrolyzes substrate. $PLD_{42/20}$ bypasses the need for anionic phospholipid to promote the conformational change that leads to disruptive interactions with the bilayer. $PLD_{42/20}$ has a higher surface hydrophobicity than PLD_{57}, based on its elution from a phenyl-Sepharose column (*8*). Also consistent with this characteristic is that the intrinsic fluorescence spectrum of $PLD_{42/20}$ is dominated by tryptophans in a more hydrophobic environment: the fluorescence emission λ_{max} is 335 nm for $PLD_{42/20}$ while that for PLD_{57} is 357 nm. Although PLD_{57} has 13 tryptophan residues, the change in intrinsic fluorescence is consistent with at least some areas of the molecule sampling a more hydrophobic environment. Incubation of PLD_{57} with increasing amounts of the soluble activator diC_4PA causes a blue shift of the emission maximum (from 357 to 335 nm). Thus, PA binding to intact PLD_{57} promotes a change such that fluorescing tryptophans are in a more hydrophobic environment. These changes in the intrinsic fluorescence spectrum of PLD_{57} binding to diC_4-PA are consistent with the ability of the PLD_{57} to enhance POPC vesicle leakiness in the presence of diC_4PA (comparable to the leakiness induced by $PLD_{42/20}$ with Ba^{2+}). It may be that diC_4PA promotes a conformational change in PLD_{57} that subsequently enhances its surface hydrophobicity at the site of membrane binding, increasing its efficiency to insert into the membrane but without causing the extensive vesicle fusion induced by $PLD_{42/20}$ in the presence of Ba^{2+} (and no PA).

The key observation is this work is that PLD-induced SUV and LUV fusion occurs without any phospholipid hydrolysis. Does this proteolytically clipped and fusogenic PLD have any counterparts in mammalian systems? Although no mammalian PLD has been suggested to be fusogenic in the absence of PA production, soluble human PLD1 has been suggested to have a role in itnracellular vesicle trafficking (*22*). Another PLD that could have similar properties is human GPI-specific PLD. That PLD is secreted from various cell types (e.g., cells of neural origin and hepatocytes) and is thought to be involved in extracellular signaling in several novel pathways as well as to have an intracellular role in some cells (*23*, *24*). GPI−PLD activated can be enhanced by proteolysis into several fragments that remain tightly associated by noncovalent interactions (*25*, *26*). Perhaps the bacterial PLD can suggest modes of action of this PLD that is also susceptible to proteolysis.

ACKNOWLEDGMENT

We thank Donald Gantz of the Boston University Biophysics Department for help with the cryo-TEM studies.

REFERENCES

1. Exton, J. H. (1997) *Physiol. Rev. 77*, 303−320.
2. Jones, D., Morgan, C., and Cockcroft, S. (1999) *Biochim. Biophys. Acta 1439*, 229−244.
3. Liscovitch, M. (1996) *J. Lipid Med. Cell Signal. 14*, 215−221.
4. McNamara, P. J., Cuevas, W. A., and Songer, J. G. (1995) *Gene 156*, 113−118.
5. McNamara, P. J., Bradley, G. A., and Songer, J. G. (1994) *Mol. Microbiol. 12*, 921−930.
6. Johansen, K. A., Gill, R. E., and Vasin, M. L. (1996) *Infect. Immun. 64*, 3259−3266.
7. Hinnebusch, J., Cherepanov, P., Du, Y., Rudolph, A., Dixon, J. D., Schwan, T., and Forsberg, A. (2000) *Int. J. Med. Microbiol. 290*, 483−487.
8. Geng, D., Baker, D. P., Foley, S. F., Stieglitz, K., and Roberts, M. F. (1999) *Biochim. Biophys. Acta 1430*, 234−244.

9. Stieglitz, K., Seaton, B., and Roberts, M. F. (1999) *J. Biol. Chem. 274*, 35367−35374.
10. Sciorra, V. A., Rudge, S. A., Prestwich, G. D., Frohman, M. A., Engebrecht, J., and Morris, A. J. (1999) *EMBO J. 18*, 5911−5921.
11. Hodgkin, M. N., Masson, M. R., Powner, D., Saqib, K. M., Ponting, C. P., and Wakelam, M. J. (2000) *Curr. Biol. 10*, 43−46.
12. Geng, D., Chura, J., and Roberts, M. F. (1998) *J. Biol. Chem. 273*, 12195−12202.
13. Zhou, C., and Roberts, M. F. (1998) *Biochemistry 37*, 16430−16439.
14. Imamura, S., and Horiuti, Y. (1979) *J. Biochem. 85*, 79−95.
15. Lowry, O. H., Rosenbrough, N. J., Farr, A. L., and Randall, R. J. (1951) *J. Biol. Chem. 193*, 265−268.
16. van Dijk, M. C., Postma, F., Hilkmann, H., Jalink, K., van Blitterswijk, W. J., and Moolenaar, W. H. (1998) *Curr. Biol. 8*, 386−392.
17. Ames, J. and Dubin, D. T. (1960) *J. Biol. Chem. 235*, 769−775.
18. Lee, G., and Pollard, H. B. (1997) *Anal. Biochem. 252*, 160−164.
19. Afdhal, N. H., Niu, N., Nunes, D. P., Bansil, R., Cao, X. X., Gantz, D., Small, D. M., and Offner, G. D. (1995) *Hepatology 22*, 856−865.
20. Poulain, F. R., Nir, S., and Hawgood, S. (1996) *Biochim. Biophys. Acta 1278*, 169−175.
21. Swairjo, M., Seaton, B. A., and Roberts, M. F. (1994) *Biochim. Biophys. Acta 1191*, 354−361.
22. Frohman, M. A., Sung, T. C., and Morris, A. J. (1999) *Biochim. Biophys. Acta 1439*, 175−186.
23. Jones, D. R., and Varela-Nieto, I. (1998) *Int. J. Biochem. Cell Biol. 30*, 313−326.
24. O'Brien, K. D., Pineda, C., Chiu, W. S., Bowen, R., and Deeg, M. A. (1999) *Circulation 99*, 2876−2882.
25. Heller, M., Butikofer, P., and Brodbeck, U. (1994) *Eur. J. Biochem. 224*, 823−833.
26. Li, J. Y., Hollfelder, K., Huang, K. S., and Low, M. G. (1994) *J. Biol. Chem. 269*, 28963−28971.

BI011338O